Quantum computation in a decoherence-free subspace with superconducting devices

Z.-Y. Xue*,[1] S.L. Zhu,[1,2] and Z.D. Wang[1]

[1]*Department of Physics and Center of Theoretical and Computational Physics, The University of Hong Kong, Pokfulam Road, Hong Kong, China*
[2]*Laboratory of Quantum Information Technology, ICMP and SPTE, South China Normal University, Guangzhou 510006, China*

We propose a scheme to implement quantum computation in decoherence-free subspace with superconducting devices inside a cavity by unconventional geometric manipulation. Universal single-qubit gates in encoded qubit can be achieved with cavity assisted interaction. A measurement-based two-qubit Controlled-Not gate is produced with parity measurements assisted by an auxiliary superconducting device and followed by prescribed single-qubit gates. The measurement of currents on two parallel devices can realize a projective measurement, which is equivalent to the parity measurement on the involved devices.

PACS numbers: 03.67.Lx Quantum computation architectures and implementations - 42.50.Dv Quantum state engineering and measurements - 85.25.Cp Josephson devices

Physical implementation of quantum computers relies on coherent and accurate evolution to achieve quantum logical gates. Recently, superconducting devices have attracted significant interest for the hardware implementation of quantum computer because of their potential scalability [1]. In addition, the cavity assisted interaction has been experimentally illustrated to have several practical advantages [2]. But, decoherence and systematic errors always occur in real quantum systems and therefore stand in the way of physical implementation. Decoherence may quickly destroy the information stored in a quantum system. Indeed, it is technically difficult for a single qubit survives for long on its own. But by teaming up, a group of qubits can work together, forming decoherence-free subspace (DFS) [3], to eliminate the influence of their environment, and thus keeping their integrity. For superconducting devices, the short dephasing time poses one of main challenges in coherent controls, and thus it is significant to figure out methods of improvement. To manipulate the quantum state, one will also inevitably encounter systematic errors. Fortunately, geometric manipulation of quantum information could result in quantum gates that are robust against stochastic control errors [4]. Combination of the resilience of the DFS approach against the environment-induced decoherence and the operational robustness of geometric manipulation was also proposed with trapped ions [5, 6] and by engineering the environment [7].

In this paper, we work out a feasible scheme to implement quantum computation based on DFS encoding with an extended unconventional geometric scenario [6, 8–10]. We illustrate our idea by incorporating the superconducting devices inside a cavity. Universal single-qubit gates in an encoded qubit [11] can be achieved with the help of cavity assisted interaction. In particular, the realization of superconducting parity measurements on two devices, together with single-device measurements and single-qubit gates, is able to generate a two-qubit Controlled-Not (CNOT) gate [12]. In this sense, this scheme is the measurement-based quantum computation. The easy combination of individual addressing and selective interaction with the many-device setup proposed in the system presents a distinct merit for physical implementation.

A device for engineering the wanted interaction is shown in Fig. 1. It consists of two superconducting quantum interference devices (SQUIDs) with a common superconducting charge box that has n excess Cooper-pair charges. Each SQUID is formed by two small identical Josephson junctions (JJs) with the capacitance C_J and Josephson coupling energy E_J, pierced by an external magnetic flux Φ_k. A control gate voltage V_g is connected to the system via a gate capacitor C_g. J_l with $l \in \{1, 2, 3, 4\}$ denotes the lth JJ. The gauge-invariant phase difference φ_l of J_l is determined from the flux quantization for the three independent loops, i.e., $\varphi_k - \varphi_{k+1} = 2\pi\Phi_k/\phi_0 \equiv 2\phi_k$ with $k \in \{1, 2, 3\}$ and $\phi_0 = h/2e$ being the flux quantum. Since we here focus on the charge regime, a convenient basis we choose is formed by the charge states, parameterized by the number of Cooper pairs n on the box with its conjugate $\varphi = \sum_l \varphi_l/4$. At temperatures much lower than the charging energy and restricting the gate charge to the range of $\bar{n} \in [0, 1]$, only a pair of adjacent charge states $\{|0\rangle, |1\rangle\}$ on the island are relevant. Setting $\phi_1 = \phi_3 = 0$, the device Hamiltonian reduces to [1]

$$H_s = -E_{ce}\sigma_z - E_\Phi\sigma_x, \quad (1)$$

where $E_\Phi = 2E_J \cos\phi_2$ and $E_{ce} = 2E_c(1-2\bar{n})$ with $E_c = e^2/2(C_g+4C_J)$ the charging energy and $\bar{n} = C_gV_g/2e$ the induced charge controlled by the gate voltage V_g.

*email: xuezhengyuan@yahoo.com.cn

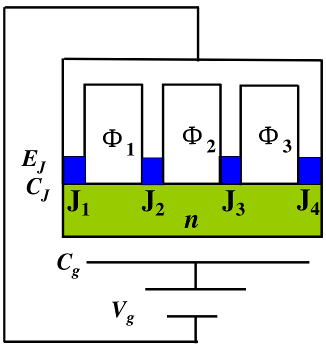

FIG. 1: Schematic illustration of the superconducting device as the effective spin. Device made of two SQUIDs with a common superconducting charge box. This more flexible design will introduce more control variables of the effective spin.

To produce the wanted interaction among devices, they are placed in a cavity, being parallel to the plane perpendicular to the magnetic component of the cavity mode, so that the cavity mode contributes an additional component to the total magnetic flux as $\varphi_t - \varphi_{t+1} = 2\phi_t + g_t(a + a^\dagger) \equiv 2\tilde{\phi}_t$, with $t \in \{1,2,3\}$ and a ($a^\dagger$) as the creation (annihilation) operator for the cavity mode. Devices are also placed at the antinodes of the cavity mode and the size of the device is negligible in comparison with the cavity mode wave length, so that the device-cavity interaction constants g_t of different devices can be treated as the same one. For simplicity, we consider only the single-mode standing wave cavity scenario, then the Hamiltonian (1) for a superconducting device in a cavity becomes

$$\begin{aligned} H_c &= -E_{ce}\sigma_z - E_J \sum_{l=1}^{4} \cos\varphi_l \\ &= -E_{ce}\sigma_z - 2E_J\left[\cos\tilde{\phi}_1 \cos\left(\frac{\varphi_1+\varphi_2}{2}\right)\right. \\ &\quad \left. + \cos\tilde{\phi}_3 \cos\left(\frac{\varphi_3+\varphi_4}{2}\right)\right] \\ &= -E_{ce}\sigma_z - E_J\left\{\left(\cos\tilde{\phi}_1 + \cos\tilde{\phi}_3\right)\right. \\ &\qquad \times\left[\cos\left(\frac{\varphi_1+\varphi_2}{2}\right) + \cos\left(\frac{\varphi_3+\varphi_4}{2}\right)\right] \\ &\quad + \left(\cos\tilde{\phi}_1 - \cos\tilde{\phi}_3\right) \\ &\qquad \left. \times\left[\cos\left(\frac{\varphi_1+\varphi_2}{2}\right) - \cos\left(\frac{\varphi_3+\varphi_4}{2}\right)\right]\right\} \\ &= -E_{ce}\sigma_z - 2E_J\left[\left(\cos\tilde{\phi}_1 + \cos\tilde{\phi}_3\right)\cos\varphi\cos\theta\right. \\ &\quad \left. + \left(\cos\tilde{\phi}_1 - \cos\tilde{\phi}_3\right)\sin\varphi\sin\theta\right], \end{aligned} \tag{2}$$

where $\theta = (\varphi_1 + \varphi_2 - \varphi_3 - \varphi_4)/4 = (\phi_1 + 2\phi_2 + \phi_3)/2 + (g_1+2g_2+g_3)(a+a^\dagger)/4$ with ϕ_1 and ϕ_3 being dc magnetic fluxes. Defining $g = (g_1+2g_2+g_3)/4$ and set $\phi_1 = \phi_3 = 0$, then $\theta = \phi_2 + g(a + a^\dagger)$. Up to the first order of g, i.e., in Lamb-Dicke limit, Hamiltonian (2) becomes

$$\begin{aligned} H_c &= -E_{ce}\sigma_z - 4E_J \cos\varphi\cos\theta \\ &\simeq H_s + 2gE_J \sin\phi_2 (a + a^\dagger)\sigma_x. \end{aligned} \tag{3}$$

We can see that the interaction can be switched off by modulating the external magnetic field as $\Phi_2 = k\phi_0$ with k an integer. In other words, the qubit and the cavity evolve independently in this case. The external flux is merely used to separately address the qubit rotations, while the evolution of the qubit is governed by Hamiltonian (1) with the coefficient E_Φ being replaced by $2E_J$.

In Ref. [13], it was assumed that the inter-SQUID loop (enclosed by the flux Φ_2 in Fig. 1) is much larger than other two SQUID loops (enclosed by the fluxes Φ_1 or Φ_3), and thus neglected the cavity mediated interaction in those loops. This would require a larger device size, and may make it more sensitive to noises. Here, we briefly elaborate that the wanted interactions among selected devices may also be induced without the loop size restriction imposed in Ref. [13]. If N devices are located within a single-mode cavity, to a good approximation, the whole system may be considered as N two-level systems coupled to a quantum harmonic oscillator [14]. Assuming the devices to work in their degeneracy points, the cavity-device interaction is given by

$$\begin{aligned} H_{int} = -2E_J \sum_{j=1}^{N} \Big[& \left(\cos\tilde{\phi}_1^j + \cos\tilde{\phi}_3^j\right)\cos\varphi_j \cos\theta_j \\ & + \left(\cos\tilde{\phi}_1^j - \cos\tilde{\phi}_3^j\right)\sin\varphi_j \sin\theta_j \Big], \end{aligned} \tag{4}$$

where we have assumed $E_J^j = E_J$ for simplicity. Assuming $g_t^j = g$, up to the first order of g, Hamiltonian (4) becomes

$$\begin{aligned} H_{int} \simeq\ & -2E_J \sum_{j=1}^{N} \Big\{ \cos\varphi_j \Big\{ \left(\cos\phi_1^j + \cos\phi_3^j\right) \\ & \times\left[\cos\phi_2^j + g\sin\phi_2^j (a+a^\dagger)\right] \\ & + g\left(\sin\phi_1^j + \sin\phi_3^j\right)(a+a^\dagger)\cos\phi_2^j \Big\} \\ & + \sin\varphi_j \Big\{ \left(\cos\phi_1^j - \cos\phi_3^j\right) \\ & \times\left[\sin\phi_2^j + g\cos\phi_2^j (a+a^\dagger)\right] \\ & + g\left(\sin\phi_1^j - \sin\phi_3^j\right)(a+a^\dagger)\sin\phi_2^j \Big\}\Big\}. \end{aligned} \tag{5}$$

Setting $\phi_2 = \omega t$ for all the selected devices and in the interaction picture with respect to

$$H_0 = \hbar\omega_c(a^\dagger a + \frac{1}{2}), \tag{6}$$

Hamiltonian (5) becomes

$$H_{int} \simeq \frac{gE_J}{2}\sum_{j=1}^{N}\left\{\sigma_j^x\left[i\left(\cos\phi_1^j+\cos\phi_3^j\right)(ae^{i\delta t}-a^\dagger e^{-i\delta t})\right.\right.$$
$$\left.-\left(\sin\phi_1^j+\sin\phi_3^j\right)(ae^{i\delta t}+a^\dagger e^{-i\delta t})\right]$$
$$-\sigma_j^y\left[\left(\cos\phi_1^j-\cos\phi_3^j\right)(ae^{i\delta t}+a^\dagger e^{-i\delta t})\right.$$
$$\left.\left.-i\left(\sin\phi_1^j-\sin\phi_3^j\right)(ae^{i\delta t}-a^\dagger e^{-i\delta t})\right]\right\} \quad (7)$$

under the rotating-wave approximation, i.e., $0 < \delta = \omega - \omega_c \ll \omega_c$. If $\phi_1 = \phi_3 = k\pi$, the cavity mediated interaction of Eq. (7) reduce to

$$H_{int}^x = i\hbar\beta\left(a^\dagger e^{-\mathrm{i}\delta t} - ae^{\mathrm{i}\delta t}\right)J_x, \quad (8)$$

where $\beta = gE_J/\hbar$ and $J_{x,y,z} = \sum_{j=1}^{N}\sigma_j^{x,y,z}$. In the case of large detuning ($\delta \gg \beta$) or periodical evolution ($\delta t = 2k\pi$), the corresponding effective Hamiltonian is given by [13–16]

$$H_x = \hbar\chi J_x^2, \quad (9)$$

where $\chi = \beta^2/\delta$. If $\phi_3 = \phi_1 - \pi = k\pi$, then the reduced effective Hamiltonian is

$$H_y = \hbar\chi J_y^2. \quad (10)$$

Note that the Hamiltonian (9) and (10) are independent on the number of devices, and can also be obtained by periodical dynamic evolution [14]. This cavity assisted collision type of Hamiltonian was first proposed for two atoms in cavity QED [16] with experimental verification in [17].

We now elucidate how to achieve universal single-qubit rotation [6]. We employ the pair-bit code by which the logical qubit is encoded in a subspace $\{|\mathbf{0}\rangle, |\mathbf{1}\rangle\}$ as

$$|\mathbf{0}\rangle_i = |0\rangle_{i_1}\otimes|1\rangle_{i_2}, \quad |\mathbf{1}\rangle_i = |1\rangle_{i_1}\otimes|0\rangle_{i_2}, \quad (11)$$

where $i = 1, \cdots, N/2$ indexes qubits of an array of N devices. Such an encoding is the well-known DFS [3] against the collective dephasing of the system-bath interaction. Let us denote X, Y, and Z as the three Pauli matrices of the encoded qubit subspace. The evolution operator for two selected devices interact with Hamiltonian in Eq. (9) is

$$U_x(\gamma) = \exp\left[-2\mathrm{i}\gamma\left(1+\sigma_{i_1}^x\sigma_{i_2}^x\right)\right]$$
$$\sim \exp\left(-2\mathrm{i}\gamma\sigma_{i_1}^x\sigma_{i_2}^x\right) = \exp\left(-2\mathrm{i}\gamma X\right), \quad (12)$$

where $\gamma = \chi t$. If we set $\phi_1 = \phi_3 = k\pi$ in device i_1 and $\phi_3 = \phi_1 - \pi = k\pi$ in device i_2, then the reduced evolution operator for the two selected devices is

$$U_y(\gamma) \sim \exp\left(-2\mathrm{i}\gamma\sigma_{i_1}^x\sigma_{i_2}^y\right) = \exp\left(-2\mathrm{i}\gamma Y\right). \quad (13)$$

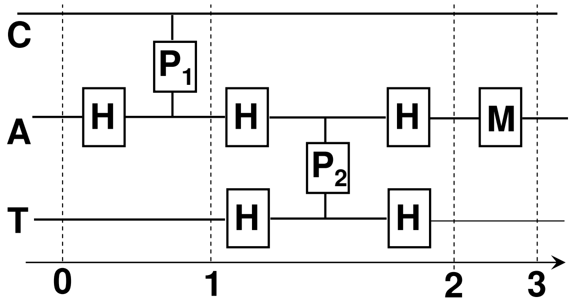

FIG. 2: Measurement-based CNOT gate for two encoded qubits. Capital letters "C" and "T" represent the control and target qubit, respectively. "A" represents an auxiliary device, it can witness the qubit state via parity measurements "P", which operate on two devices, one from "A" and the other from "C" or "T". "H" is the Hadamard gate. The measurement "M" results of "A" in the $\{|0\rangle, |1\rangle\}$ basis together with the outcomes of the two parity measurements "P" determine which operation one has to apply on the "C" and "T" qubit in order to complete the CNOT gate. The arrowed line in the bottom represents the sequence of the process. The point "0", "1", "2", and "3" stand for the initial system state, the system states after measurements "P_1", before and after "M", respectively.

Certainly, (12) and (13) are non-commutable, constructing the well-known universal single-qubit rotations.

We next proceed to implement a CNOT gate between two encoded qubits with the help of an auxiliary device. Here we propose a measurement-based CNOT gate operation [12]. The relevant operations are single-qubit rotations, single-device rotations/measurements, and effective parity measurements for two devices. The circuit for the CNOT gate is depicted in Fig. 2. The auxiliary device is initially prepared in its ground state $|0\rangle_A$. The parity measurement is operated in $\{|0\rangle, |1\rangle\}$ basis. The devices can be treated as effective spin 1/2 systems, and the parity here represents for the total spin for the two involved devices, which can be used to witness the states of the involved spins [12]. After a Hadamard gate on the auxiliary device, the first parity measurement P_1 in Fig. 2 is implemented on the auxiliary device and the first device from "C" qubit. After Hadamard rotation of the auxiliary devices and the target qubit, the second parity measurement P_2 is implemented on the auxiliary device and the first device in the "T" qubit. Then we rotate back the auxiliary device and the target qubit state by Hadamard gate. The last step is the measurement of the auxiliary device in the $\{|0\rangle, |1\rangle\}$ basis. The two parity measurement results, together with the measurement result of the auxiliary device determine which single-qubit gates to be operated on the control and target qubits to generate a CNOT gate. The relationship between the measurement results and the gates to be operated is summarized in the table I. After completing the required gates on the corresponding qubits, it is straightforward

TABLE I: Table of the correspondence between the measurement results and the gates operated on the control and target qubits. "0" and "1" represent odd and even parity, respectively.

"P_1"	"P_2"	result of "M"	gate on "C"	gate on "T"
1	1	$\|0\rangle_A$	I	I
1	1	$\|1\rangle_A$	I	X
1	0	$\|0\rangle_A$	Z	I
1	0	$\|1\rangle_A$	Z	X
0	1	$\|0\rangle_A$	I	X
0	1	$\|1\rangle_A$	I	I
0	0	$\|0\rangle_A$	Z	X
0	0	$\|1\rangle_A$	Z	I

to check that the process is a CNOT gate operation between the two qubits.

To verify that a CNOT gate is implemented after the circuit plotted in Fig. 2, we consider that the two qubits are initially in the states

$$|\psi\rangle_C = (\alpha|\mathbf{0}\rangle + \zeta|\mathbf{1}\rangle)_C\,, \tag{14a}$$

$$|\psi\rangle_T = (\xi|\mathbf{0}\rangle + \tau|\mathbf{1}\rangle)_T\,, \tag{14b}$$

where $|\alpha|^2+|\zeta|^2 = 1$ and $|\xi|^2+|\tau|^2 = 1$. The initial state of the system at point 0 in Fig. 2 is given by

$$|\psi\rangle_C \otimes |0\rangle_A \otimes |\psi\rangle_T. \tag{15}$$

The circuit in Fig. 2, together with prescribed single-qubit gates, is to ensure the final state to be

$$\alpha|\mathbf{0}\rangle_\mathbf{C}\,(\xi|\mathbf{0}\rangle + \tau|\mathbf{1}\rangle)_\mathbf{T} + \zeta|\mathbf{1}\rangle_\mathbf{C}\,(\xi|\mathbf{1}\rangle + \tau|\mathbf{0}\rangle)_\mathbf{T}\,, \tag{16}$$

up to a global phase. For the sake of definitiveness, let us single out one of the possibilities as an example. If $P_1 = 0$, the system state at point 1 reduces to

$$(\alpha|\mathbf{0}\rangle_C|1\rangle_A + \zeta|\mathbf{1}\rangle_C|0\rangle_A) \otimes |\psi\rangle_T. \tag{17}$$

If $P_2 = 1$, the system state at point 2 is

$$\begin{aligned}\frac{1}{2}\{\alpha|\mathbf{0}\rangle_\mathbf{C}&[(\tau+\xi)(|\mathbf{0}\rangle+|\mathbf{1}\rangle)_\mathbf{T}\otimes|\psi\rangle_\mathbf{A}\\ &+(\tau-\xi)(|\mathbf{0}\rangle-|\mathbf{1}\rangle)_\mathbf{T}\otimes|\bar{\psi}\rangle_\mathbf{A}]\\ +\zeta|\mathbf{1}\rangle_\mathbf{C}&[(\xi+\tau)(|\mathbf{0}\rangle+|\mathbf{1}\rangle)_\mathbf{T}\otimes|\psi\rangle_\mathbf{A}\\ &+(\xi-\tau)(|\mathbf{0}\rangle-|\mathbf{1}\rangle)_\mathbf{T}\otimes|\bar{\psi}\rangle_\mathbf{A}]\}.\end{aligned} \tag{18}$$

where $|\psi\rangle_A = (|0\rangle+|1\rangle)_A/\sqrt{2}$ and $|\bar{\psi}\rangle_A = (|0\rangle-|1\rangle)_A/\sqrt{2}$. If the measurement result of the auxiliary devices is $|0\rangle_A$, the system state at point 3 is

$$\alpha|\mathbf{0}\rangle_\mathbf{C}(\tau|\mathbf{0}\rangle + \xi|\mathbf{1})_\mathbf{T} + \zeta|\mathbf{1}\rangle_\mathbf{C}(\xi|\mathbf{0}\rangle + \tau|\mathbf{1}\rangle)_\mathbf{T}, \tag{19}$$

which relates to the targeted final state (16) up to a X-gate on the target qubit (c.f. the table). Thus a nontrivial two-qubit CNOT gate is achieved.

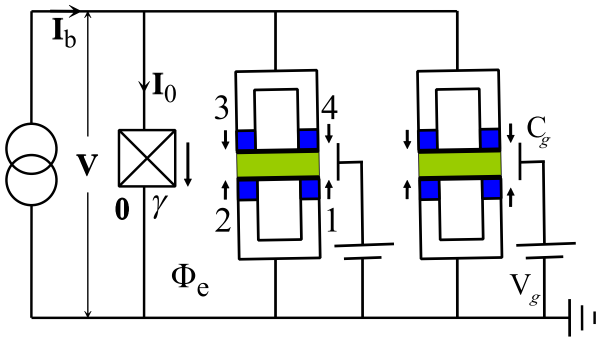

FIG. 3: A Josephson-Junction circuit with one large junction "0" and two parallel charge devices. One of the devices is from the encoded qubit and the other is its auxiliary device. Each device consists of two SQUID loops. The small arrow near each JJ denotes the direction of its phase drop. Φ_e is the dc external magnetic flux of the loop consists of junction "0" and the first device, which are related to the inter-SQUID magnetic flux of the devices, and the cavity mediated interaction can be neglected in this situation. The external magnetic flux of the SQUID loops in both devices are set to be zero during the parity measurement.

At this stage, we elaborate how to implement a parity meter for superconducting devices [18–20]. Let us consider a circuit with one large junction denoted by "0" and two parallel devices (c and t) made up of smaller JJs, as shown in Fig. 3 [19]. Under an external bias current I_b, the current flowing through the large junction may be written as

$$I_0 = |I_b + I_d| = \left|I_b + \langle\psi_{1,2}|\hat{I}|\psi_{1,2}\rangle\right| \tag{20}$$

where $\hat{I}$ is the current operator for the two parallel devices and I_d is the sum of their expectation values. If $I_0 > I_c$ with I_c as the critical current of the large junction, the large junction is switched from the superconducting state (with zero voltage across the junction) to the normal state (with a nonzero voltage V). As $\hat{I}$ is related to the device's state, by monitoring the voltage across the junction one can determine which type of state those JJ devices have been projected to [18], and thus realize a quantum-state selector [19, 20] (see below for details). If I_b is set to be significantly smaller than I_c and given the fact that $I_d \ll I_b$, then I_0 will always be less than I_c, i.e., no measurement is in effect. Therefore, by a proper choice of the bias current I_b, we are able to realize effectively switching on/off of the process.

It is notable that the device in Fig. 3 is the same as that of in Fig. 1. In Fig. 3, we have chosen the magnetic flux of SQUID loops, Φ_1 and Φ_3 in Fig. 1, to be zero in each device, which simplifies our calculation [19]. With such choice, the constrain of the inter-SQUID loop for each device is $\varphi_2 - \varphi_3 = \varphi_1 - \varphi_4 = 2\pi\Phi_e/\phi_0 - \gamma$, i.e., $\Phi_2 \equiv 2\pi\Phi_e/\phi_0 - \gamma$ for both devices, where γ is the gauge phase drop of the large JJ. For the two-device case, setting $\Phi_e = \phi_0/2$, the total current operator of both parallel devices is given by [19]

$$\hat{I} = I_1\sigma_x^1 + I_2\sigma_x^2, \tag{21}$$

which is state-dependent with $I_{1(2)}$ being the critical current of the SQUID in device 1(2). To implement the parity measurement, we choose $I_b = I_c - (I_1 + I_2)/2$ [20], i.e.,

$$I_0 = I_c - (I_1 + I_2)/2 + \langle\psi_{1,2}|\hat{I}|\psi_{1,2}\rangle. \tag{22}$$

Denote states $|\pm\rangle$ as the eigenstates of σ_x with eigenvalues ±1, i.e., $\sigma_x|\pm\rangle = \pm|\pm\rangle$. If $\psi_{1,2} = |+\rangle_1|+\rangle_2$, then

$$I_0 = I_c + \frac{I_1 + I_2}{2} > I_c, \tag{23}$$

therefore the large junction is switched from the superconducting state to the normal state with a nonzero voltage V_1. For the other three cases $\psi_{1,2} \in \{|+\rangle_1|-\rangle_2, |-\rangle_1|+\rangle_2, |-\rangle_1|-\rangle_2\}$, it is direct to check $I_0 < I_c$. In other words, if $V_1 \neq 0$, the projective measurement

$$P_1' = |+\rangle_1|+\rangle_{2,2}\langle+|_1\langle+| \tag{24}$$

is implemented on the two involved devices. For $V_1 = 0$, we may reverse both the external field Φ_e and bias current I_b to their opposite directions, and monitor the voltage again. If $V_2 \neq 0$, then

$$P_2' = |-\rangle_1|-\rangle_{2,2}\langle-|_1\langle-| \tag{25}$$

is implemented. If $V_2 = 0$ again, this corresponds to the measurement

$$P_3' = |+\rangle_1|-\rangle_{2,2}\langle+|_1\langle-| + |-\rangle_1|+\rangle_{2,2}\langle-|_1\langle+|. \tag{26}$$

It is obvious that P_1' and P_2' are even parity, while P_3' is odd parity. This constructs a superconducting parity meter in the $\{|\pm\rangle\}$ basis. Rotation of the device state before and after the measurement results in the parity meter in the $\{|0\rangle, |1\rangle\}$ basis, which is adopted in our implementation of the CNOT gate. It is also needed to measure the auxiliary devices in the present implementation of the CNOT gate, which can also be achieved with a minor modification of the setup [19].

We now briefly address the experimental feasibility of our scheme. Individual addressability is normally a prerequisite in any quantum manipulation. Here, the size of the device setup is macroscopic, thus individual addressability is taken as granted. Meanwhile, local controllability of single qubit is obtained by conventional methods [1]. The cavity-device coupling and decoupling can be controlled by the external magnetic flux, which can be effectively controlled. This also ensures the selective cavity-device interaction. In addition, the implementation set the devices working in their degeneracy points, where they possess long coherence time and minimal charge noises. Typical gate operation time is $t \sim 10$ ns [14], which is much shorter than both the lifetime of qubit and cavity decay time (at least on the order of μs [1, 16]). Imperfect control of time results in the fluctuation of periodical condition while cavity decay forbids the cavity state back to the original point in phase space, this contribute to the decoherence in current implementation. However, detailed examinations [21–23] show that these will only result a little bit infidelity of the gate operation.

In summary, we have proposed a feasible scheme to implement quantum computation in the DFS with superconducting devices inside a cavity. The wanted interaction between selective devices can be implemented. Universal single-qubit gates can be achieved with cavity assisted interaction. A measurement-based two-qubit CNOT gate is produced with parity measurements assisted by an auxiliary device and followed by prescribed single-qubit gates. The easy combination of individual addressing and selective interaction with the many-device setup proposed in the system presents a distinct merit for our physical implementation.

This work was supported by the RGC of Hong Kong under Grants Nos. HKU7045/05P and HKU7049/07P plus HKU7044/08P, the NSFC under Grants No. 10429401 and No. 10674049, and the State Key Program for Basic Research of China (No. 2006CB921800 and No. 2007CB925204).

[1] J. Q. You and F. Nori, Phys. Today **58** (11) (2005) 42; Y. Makhlin, G. Schön, and A. Shnirman, Rev. Mod. Phys. **73** (2001) 357 .
[2] A. Wallraff, D. I. Schuster, A. Blais, L. Frunzio, R.-S. Huang, J. Majer, S. Kumar, S. M. Girvin, and R. J. Schoelkopf, Nature (London) **431** (2004) 162.
[3] L.-M. Duan and G. C. Guo, Phys. Rev. Lett. **79** (1997) 1953; P. Zanardi and M. Rasetti, Phys. Rev. Lett. **79** (1997) 3306; D. A. Lidar, I. L. Chuang, and K. B. Whaley, Phys. Rev. Lett. **81** (1998) 2594 .
[4] S.-L. Zhu and P. Zanardi, Phys. Rev. A **72** (2005) 020301(R).
[5] L.-A. Wu, P. Zanardi, and D. A. Lidar, Phys. Rev. Lett. **95** (2005) 130501; X. D. Zhang, Q. H. Zhang, and Z. D. Wang, Phys. Rev. A **74** (2006) 034302.
[6] L.-X. Cen, Z. D. Wang, and S. J. Wang, Phys. Rev. A **74** (2006) 032321.
[7] A. Carollo, M. França Santos, and V. Vedral, Phys. Rev. Lett. **96** (2006) 020403; Z.-Q. Yin, F.-L. Li, and P. Peng, Phys. Rev. A **76** (2007) 062311.
[8] D. Leibfried, B. DeMarco, V. Meyer, D. Lucas, M. Barrett, J. Britton, W.M. Itano, B. Jelenkovic, C. Langer, T. Rosenband, and D.J.Wineland, Nature (London) **422** (2003) 412.
[9] S.-L. Zhu and Z.D. Wang, Phys. Rev. Lett. **91** (2003) 187902; J. Du, P. Zou, and Z. D. Wang, Phys. Rev. A **74** (2006) 020302.

[10] S. B. Zheng, Phys. Rev. A **70** (2004) 052320; Phys. Rev. A **74** (2006) 032322.

[11] In order to avoid confusion, we use "qubit" to denote the encoded logical qubit, while "device" for the superconducting charge qubit schemeticed in Fig. 1 through out this paper.

[12] O. Zilberberg, B. Braunecker, and D. Loss, Phys. Rev. A **77** (2008) 012327.

[13] Z.-Y. Xue, Z. D. Wang, and S.-L. Zhu, Phys. Rev. A **77** (2008) 024301.

[14] S.-L. Zhu, Z. D. Wang, and P. Zanardi, Phys. Rev. Lett. **94** (2005) 100502; Z.-Y. Xue and Z. D. Wang, Phys. Rev. A **75** (2007) 064303.

[15] A. Sørensen and K. Mølmer, Phys. Rev. A **62** (2000) 022311.

[16] S.-B. Zheng and G.-C. Guo, Phys. Rev. Lett. **85** (2000) 2392; S.-B. Zheng, Phys. Rev. A **66** (2002) 060303(R).

[17] S. Osnaghi, P. Bertet, A. Auffeves, P. Maioli, M. Brune, J. M. Raimond, and S. Haroche, Phys. Rev. Lett. **87**, 037902 (2001).

[18] D. Vion, A. Aassime, A. Cottet, P. Joyez, H. Pothier, C. Urbina, D. Esteve, and M. H. Devoret, Science **296** (2002) 886.

[19] J. Q. You, J. S. Tsai, and F. Nori, Phys. Rev. Lett. **89** (2002) 197902; Phys. Rev. B **68** (2003) 024510.

[20] X.-B. Wang, J. Q. You, and F. Nori, Phys. Rev. A **77** (2008) 062339; quant-ph/0608205 (2006).

[21] S.-B. Zheng, Phys. Rev. Lett. **95** (2005) 080502.

[22] C.-Y. Chen et al., Phys. Rev. A **73** (2006) 032344; ibid. **74** (2006) 032328.

[23] Z.-G. Shi, X.-W. Chen, and K.-H. Song, J. Phys. B: At. Mol. Opt. Phys. **42** (2009) 035504.